Research Square

Preprints are preliminary reports that have not undergone peer review.
They should not be considered conclusive, used to inform clinical practice,
or referenced by the media as validated information.

Triflusal targeting COX-1 suppresses HBV infection in vitro and in vivo

Huijing Ruan
Tongji Medical College of Huazhong University of Science and Technology
Kai Yang
Tongji Medical College of Huazhong University of Science and Technology
Mingzhe Yan
Tongji Medical College of Huazhong University of Science and Technology
Xiaojian Tan
Tongji Medical College of Huazhong University of Science and Technology
Wenyuan Zhang
Tongji Medical College of Huazhong University of Science and Technology
Jisong Yan
Chinese Academy of Medical Sciences & Peking Union Medical College
Jie Zhou
Tongji Medical College of Huazhong University of Science and Technology
Bei Ye
Tongji Medical College of Huazhong University of Science and Technology
Jie Xiang
Tongji Medical College of Huazhong University of Science and Technology
Qingyu Yang
Tongji Medical College of Huazhong University of Science and Technology
Lianguo Ruan
2020jy0004@hust.edu.cn

Tongji Medical College of Huazhong University of Science and Technology

Research Article

Keywords: Hepatitis B virus, Antivirals, triflusal, COX-1, cAMP/PKA/CREB signaling pathway

Posted Date: March 5th, 2026

DOI: https://doi.org/10.21203/rs.3.rs-8928353/v1

License: This work is licensed under a Creative Commons Attribution 4.0 International License.
Read Full License

Additional Declarations: No competing interests reported.

Abstract

Background: Chronic hepatitis B virus infection poses a persistent global public health burden with limited therapeutic options, and host-targeted antiviral strategies are urgently needed. Cyclooxygenase-1, encoded by the *PTGS1* gene, has emerged as a potential host factor regulating viral replication, while triflusal, a specific COX-1 inhibitor, modulates intracellular cyclic adenosine monophosphate levels and its anti-HBV activity remains uncharacterized.

Methods: Huh7 cells were transfected with gradient doses of HBV 1.3-fold overlength plasmid and treated with triflusal (0–20 μM). Real-time quantitative PCR was used to detect *PTGS1* mRNA and HBV 3.5-kb RNA levels; enzyme-linked immunosorbent assay measured hepatitis B surface antigen, hepatitis B e antigen and intracellular cAMP levels. MTT assay assessed triflusal cytotoxicity. *PTGS1* overexpression and siRNA knockdown were performed to verify its role in HBV replication. An acute HBV mouse model (AAV-HBV1.3) was used to evaluate in vivo anti-HBV efficacy of triflusal (30/50 mg/kg). Western blot and functional assays explored the involvement of the cAMP/protein kinase A (PKA)/cAMP response element-binding protein (CREB) signaling pathway.

Results: *PTGS1* mRNA expression and HBV replication markers (3.5-kb RNA, HBsAg, HBeAg) were upregulated in a plasmid dose-dependent manner in HBV-transfected Huh7 cells. Triflusal inhibited HBV antigen secretion and 3.5-kb RNA transcription in a concentration-dependent manner in vitro, with no obvious cytotoxicity at effective antiviral doses. *PTGS1* overexpression enhanced HBV replication, while its knockdown suppressed viral markers, confirming a positive correlation between *PTGS1* and HBV replication. Triflusal treatment elevated intracellular cAMP levels by inhibiting COX-1/TXA_2 signaling, activating the PKA/CREB pathway, which suppressed HBV core promoter activity and disrupted viral core particle assembly. In vivo, triflusal significantly reduced serum HBeAg and hepatic HBV 3.5-kb RNA levels in HBV-infected mice, with good biocompatibility and no acute toxicity.

Conclusions: Triflusal exerts potent anti-HBV effects in vitro and in vivo by targeting COX-1 to activate the cAMP/PKA/CREB signaling pathway, which suppresses HBV replication at both transcriptional and post-transcriptional levels. Our findings identify COX-1 as a promising host-directed therapeutic target for HBV infection and provide a theoretical basis for repurposing triflusal as a novel adjunctive treatment for chronic HBV infection.

Background

Hepatitis B virus (HBV) infection is a major global public health challenge. HBV, a DNA virus, can lead to chronic hepatitis, liver fibrosis, cirrhosis, and hepatocellular carcinoma[1–2]. According to the World Health Organization (WHO), approximately 296 million people worldwide are chronically infected with HBV. As a country with a high HBV infection burden, China faces a particularly severe situation. Based on the 2024 WHO Hepatitis Report, the prevalence of hepatitis B surface antigen (HBsAg) in China is approximately 5.6%, accounting for 31.5% of global cases and 82.2% of cases in the Asia-Pacific

region[3–4]. Despite significant preventive progress through large-scale vaccination programs, approximately 75 million individuals currently live with chronic HBV infection in China. Annually, about 308,000 people die from HBV-related liver diseases in China, accounting for over 30% of global HBV-related deaths, highlighting a persistent, substantial disease burden[5].

Currently, clinical management of chronic hepatitis B (CHB) primarily relies on nucleos(t)ide analogues such as entecavir (ETV), tenofovir (TDF), and interferon [5–7] However, prolonged treatment can result in drug resistance, particularly with lamivudine, which has a resistance rate exceeding 70% after five years of use[8]. Additionally, these medications can have significant adverse effects, such as nephrotoxicity and decreased bone density associated with TDF[9]. The ultimate goal of HBV treatment is the eradication of HBsAg; unfortunately, current therapeutic agents rarely achieve this outcome[8 –9]. Therefore, there is an urgent need to identify anti-HBV drugs with novel mechanisms of action.

In recent years, researchers have begun exploring older drugs with immunomodulatory or cell-signaling regulatory effects as potential treatments for HBV infection. The small-molecule compound triflusal (2-acetoxy-4-trifluoromethylbenzoic acid), a known antiplatelet agent, inhibits cyclooxygenase-1 (COX-1) and modulates intracellular cyclic adenosine monophosphate (cAMP) levels[11–12]. Drug triflusal has been used for decades in cardiovascular diseases and possesses a unique dual mechanism involving COX-1 acetylation and phosphodiesterase (PDE) inhibition, thereby regulating intracellular cAMP levels[14–15]. The cAMP signaling pathway plays a complex and critical role in viral infection and replication[15–16]. In HIV-infected cells, cAMP inhibits viral promoter transcriptional activity and reduces viral DNA transport from the cytoplasm to the nucleus[17–18]. Studies have revealed that epigenetically regulated miR-449a enhances HBV replication by targeting cAMP response element-binding protein 5 (CREB5)[19], highlighting a significant link between the cAMP pathway and HBV replication. Furthermore, COX-1 has been identified as essential for efficient viral replication; for example, simultaneous inhibition of COX-1 and COX-2 significantly reduced viral yields in herpes simplex virus type 1 (HSV-1) infection[20]. Additionally, research indicates that COX-1 plays a crucial role in the body temperature response and disease progression during influenza A virus infection in mice, with COX-1 deficiency leading to increased morbidity and inflammation[21]. The cAMP response element (CRE) and the ATF/CREB transcription factor family also participate in regulating replication and pathogenesis of various human viruses, including HBV[22]. Collectively, these findings provide a theoretical foundation for exploring the anti-HBV potential of triflusal through modulation of the COX-1-cAMP signaling axis.

Compound triflusal suppresses inflammatory responses by inhibiting COX-1 acetylation, and chronic inflammation is a key driver in the progression of HBV infection to cirrhosis and hepatocellular carcinoma. Additionally, its ability to elevate intracellular cAMP levels through phosphodiesterase (PDE) inhibition may directly affect HBV replication. Previous studies have shown that cAMP suppresses viral promoter transcriptional activity and reduces nuclear transport of viral DNA[22], which is particularly relevant for HBV, as its replication requires the formation of covalently closed circular DNA (cccDNA) in the nucleus.

In this study, The small-molecule compound triflusal was identified through phenotypic screening. This compound reduced HBsAg levels and decreased HBV RNA expression. We further investigated the molecular mechanisms by which triflusal inhibits HBV replication, aiming to provide experimental evidence to support the development of novel anti-HBV therapeutic strategies.

Materials and Methods

Cell Lines, Plasmids, and Compounds

The cell lines used in this study included Huh7 (human hepatocellular carcinoma cell line), HepG2 (human hepatocellular carcinoma cell line), and HCCLM3 (hepatocellular carcinoma with lymph node metastasis-3) cells, provided by Professor Jianguo Wu. Cells were cultured in high-glucose Dulbecco's Modified Eagle's Medium (DMEM; HyClone, UT, USA) supplemented with 10% fetal bovine serum (FBS; HyClone, UT, USA) and 1% penicillin/streptomycin (Invitrogen, Carlsbad, CA, USA) at 37°C in a humidified incubator containing 5% CO_2. Compound triflusal was purchased from Selleck Chemicals (S3200, Houston, TX, USA).

The plasmid pBlue-HBV1.3, which expresses HBV RNA, was used for transfection experiments. Specific small interfering RNAs (siRNAs) targeting human COX-1 (siRNA sequence: 5'-GCATTGCCATGGAGTTCAA-3') and a scrambled negative control siRNA (NC-siRNA sequence: 5'-UUCUCCGAACGUGUCACGUTT-3') were synthesized by GenePharma. Compound triflusal was selected as the investigational agent due to its known target, COX-1, encoded by the *PTGS1* gene.

MTT Assay

To assess the cytotoxicity of triflusal in HepG2 and Huh7 cells, cell viability was evaluated using the MTT assay[23–24]. Cells were seeded in 96-well plates at a density of 5×10^3 cells per well and cultured in DMEM supplemented with 10% FBS. After 24 hours, cells were treated with serial dilutions of triflusal (ranging from 100 μM to 0.006 μM) or left untreated for 72 hours. The medium was then removed, and MTT solution (0.5 mg/mL) was added to each well and incubated for 4 hours. Subsequently, dimethyl sulfoxide (DMSO) was added to dissolve the formazan crystals, and absorbance was measured at 490 nm using a microplate reader (TECAN Infinite F50, China), with a reference wavelength of 620 nm[26]. Cytotoxicity was expressed as the 50% cytotoxic concentration (CC_{50}), calculated using nonlinear regression analysis with GraphPad Prism 10.0. All experiments were performed in triplicate and repeated independently three times.

RNA Extraction and Quantitative Real-Time PCR

Total RNA was extracted from cell or tissue samples using a total RNA extraction kit (Cat. DP424b, China) according to the manufacturer's instructions. Subsequently, cDNA was synthesized using random

hexamer primers and reverse transcriptase (Cat. M1701, Promega, Madison, WI, USA). Real-time quantitative PCR (qPCR) was performed using SYBR Green Supermix on the StepOnePlus system under the following conditions: 95°C for 5 min, followed by 40 cycles of 95°C for 15 s and 60°C for 15 s. Primer sequences included HBV 3.5-kb RNA, human GAPDH (hGAPDH), and mouse GAPDH (mGAPDH). Gene expression levels were quantified using the $2^{-\Delta\Delta Ct}$ method, with GAPDH as the internal control.

Quantification of HBsAg and HBeAg by ELISA

Levels of HBsAg and hepatitis B e antigen (HBeAg) (Wantai, Beijing, China) in cell culture supernatants were determined using sandwich enzyme-linked immunosorbent assays (ELISA), as previously described. Briefly, 100 µL of cell culture supernatant (appropriately diluted in sample diluent, if necessary) was added to microtiter plates pre-coated with anti-HBsAg or anti-HBeAg antibodies and incubated at 37°C for 60 min. Following five washes, 100 µL of horseradish peroxidase (HRP)-conjugated detection antibody was added to each well and incubated at 37°C for 15–30 min. After additional washes, 100 µL of 3,3',5,5'-tetramethylbenzidine (TMB) substrate was added, and plates were incubated at room temperature for 15–30 min. The reaction was stopped by adding 100 µL of stop solution, and optical density (OD) values were measured at 450 nm (reference wavelength: 630 nm) using a microplate reader (TECAN Infinite F50, China)[28].

ELISA

Detection of HBsAg and HBeAg was performed using an HBV ELISA Kit (Aviva Systems Biology), and intracellular cAMP levels were measured using a cAMP ELISA Kit (Jiangsu Enzyme Immunoassay). For HBsAg and HBeAg detection, a sandwich immunoassay was employed, where capture antibodies were coated onto microplate wells. After sample addition, antigens bound to capture antibodies. After washing, enzyme-labeled detection antibodies were added to form an antibody-antigen-enzyme-labeled antibody complex. TMB substrate was added for color development, with color intensity directly proportional to antigen concentration. For cAMP detection, a competitive assay was performed, where sample cAMP competed with enzyme-labeled cAMP for limited antibody binding sites. Following binding, substrate was added, and color intensity was inversely proportional to sample cAMP concentration.

Western Blot Analysis

Cells were pre-chilled, washed with phosphate-buffered saline (PBS), and lysed on ice for 60 min using western blot lysis buffer (Cat: BL509A, Biosharp, China) containing a protease inhibitor cocktail (CAS: 56-25-7, Roche, Switzerland). Samples were denatured by boiling, and proteins were separated using a Bio-Rad electrophoresis system before transfer onto nitrocellulose (NC) membranes (Cat: HATF00010, Millipore, Billerica, MA, USA). Membranes were blocked with PBST containing 5% skim milk powder for 1 h and incubated overnight at 4°C with primary antibodies (1:1000 dilution). After three washes with

PBST, membranes were incubated for 1 h at room temperature with corresponding HRP-conjugated secondary antibodies (1:5000 dilution). Following washing, protein bands were visualized using SuperSignal West Pico chemiluminescent substrate (CLiN, Shenzhen, China). Antibodies used were as follows: COX-1 (Cat: 13393-1, Proteintech, China), HBc (Cat: ab8637, Abcam, China), β-actin (Cat: 60008-1, Proteintech, China), goat anti-rabbit IgG (Cat: SA00001-2, Proteintech, China), and goat anti-mouse IgG (Cat: SA00001-1, Proteintech, China).

HBV Mouse Model

Six- to seven-week-old male C57BL/6J mice were purchased from Beijing Vital River Laboratory Animal Technology Co., Ltd. (Beijing, China) and housed in a specific pathogen-free (SPF) environment. An acute HBV infection model was established via tail vein injection of adeno-associated virus (AAV)-HBV1.3 plasmid encoding 1.3 copies of the HBV genome (genotype B, serotype adw) packaged in AAV serotype 8 capsids.

The control group received an equal volume of phosphate-buffered saline (PBS). Mice were randomly divided into 5 groups (n = 8 per group): normal control, model control, low-dose treatment (30 mg/kg), high-dose treatment (50 mg/kg), and drug control. Treatment groups received oral administration daily for 5 consecutive days. Blood and liver tissue samples were collected on days 5 and 14 post-infection. A portion of liver tissue was frozen at -80°C, while the remaining tissue was fixed in 4% paraformaldehyde for paraffin embedding and sectioning. Hematoxylin-eosin (HE) staining was conducted to evaluate pathological changes, and immunohistochemistry was performed to detect HBV antigen expression.

Ethics Statement

C57BL/6J mice (aged 6–7 weeks) were housed under pathogen-free conditions at Beijing Vital River Laboratory Animal Technology Co., Ltd. (Beijing, China) throughout the experimental period. Standard housing and environmental conditions were strictly maintained. All animal procedures and husbandry practices were performed in accordance with guidelines approved by the Animal Care and Use Committee of the Wuhan Institute of Virology (Approval No.: WIVA38202103).

Statistical Analysis

Statistical analyses were performed using GraphPad Prism 8 software. Experimental data are presented as means ± standard deviations (SD). Statistical comparisons between groups were conducted using paired-sample t-tests, with a significance threshold set at $p < 0.05$. To ensure the reliability of results, all experiments were independently repeated three times.

Results

Screening for Anti-HBV Small-Molecule Inhibitors

Discovery of Compound triflusal as an HBV replication inhibitor. Initial screening of 7,000 compounds at 20 μM concentration in a 96-well plate format identified two compounds capable of reducing HBV surface antigen (HBsAg) levels by more than 50% compared with mock-treated controls. Subsequent cytotoxicity testing revealed compound triflusal (Fig. 1B) exhibited the greatest potential anti-HBV activity. To clarify cytotoxic effects, median cytotoxic concentrations (CC_{50}) of triflusal were determined in LM3, HepG2, and Huh7 cells. The average CC_{50} values were 122.8 μM (Fig. 1C), 112.2 μM (Fig. 1D), and 60.58 μM (Fig. 1E), respectively.

In Vitro Suppression of HBV by Compound triflusal

To evaluate the antiviral activity of compound triflusal at the cellular level, a series of assays were conducted using Huh7 cells transiently transfected with the HBV1.3 plasmid[27]. The results demonstrated that triflusal significantly inhibited HBV antigen expression and mRNA transcription in a concentration-dependent manner. At concentrations of 0.8, 4, and 20 μM, compound triflusal reduced HBeAg secretion by approximately 87.91% (Fig. 2A), and inhibited HBsAg secretion by approximately 71.5% at 20 μM (Fig. 2D). The inhibitory effect on HBeAg was slightly stronger than on HBsAg (Fig. 2B, E). To further evaluate the antiviral triflusal effect, HBV 3.5-kb RNA levels were quantified by qPCR. Expression of HBV 3.5-kb RNA was suppressed by triflusal in HBV1.3-transfected Huh7 cells in a dose-dependent manner (Fig. 2C, F), consistent with reduced HBsAg and HBeAg levels detected by ELISA.

Huh7 cells were untransfected or transfected with 1 μg HBV1.3, then treated with serially diluted triflusal (0.8, 4, 20 μM) for 30 h. HBV 3.5 kb mRNA level was detected by qPCR (A). HBeAg and HBsAg levels were measured by ELISA (B, C), and inhibition rates were calculated (D-F). *$p < 0.05$, **$p < 0.01$, ***$p < 0.001$.

Relative RNA levels in cells treated with 0.8, 4, and 20 μM concentrations decreased to approximately 0.65, 0.15, and 0.60, respectively, with an inhibition rate of approximately 40.4% at 20 μM (Fig. 2C, F) triflusal. Collectively, these data demonstrate that compound triflusal effectively inhibits HBV replication in vitro by suppressing HBV RNA transcription and antigen expression, highlighting its potential as an anti-HBV candidate drug. All differences between experimental and control groups were statistically significant (*$P < 0.05$, **$P < 0.01$, *$P < 0.001$).

In Vivo Suppression of HBV by Compound triflusal

The *in vivo* therapeutic effects of compound triflusal were evaluated using a hydrodynamic injection (HDI)-based HBV mouse model. The safety profile of triflusal was also assessed; no significant changes in body weight were observed in any treatment group compared to the model control group throughout the experimental period, indicating good biocompatibility and absence of acute overt toxicity at tested doses. Mice were randomly divided into five groups: blank control, untreated model, low-dose treatment (30 mg/kg), high-dose treatment (50 mg/kg), and positive drug groups. After a 3-day adaptation period, mice received injections of pAAV-HBV1.2 plasmid on Day 0, while the control group received an equal

volume of PBS. A single intravenous administration of compound triflusal (30 and 50 mg/kg) was given 6 hours after HDI with the HBV plasmid, eliciting a robust antiviral response (Fig. 3A). Serum and liver samples were collected and analyzed for HBeAg at 5 and 14 days post-treatment. Consistent with in vitro findings, mice treated with compound triflusal exhibited significantly reduced serum HBeAg levels compared to untreated controls (Fig. 3C, D). Additionally, HBV RNA isolated from liver tissues showed that the levels of HBV RNA intermediates in mice treated with compound triflusal decreased to approximately 20–50% of those observed in untreated controls (Fig. 3C, D).

The Role of PTGS1 in triflusal-Mediated HBV Suppression

Previous studies suggested that *PTGS1* is essential in regulating cAMP metabolism, thereby influencing viral replication. Therefore, we investigated the role of *PTGS1* in the anti-HBV effects mediated by compound triflusal. Increasing HBV1.3 plasmid transfection in Huh7 cells resulted in a dose-dependent upregulation of HBV markers and *PTGS1* mRNA (Fig. 5A-D). Overexpression of *PTGS1* further enhanced HBV replication (Fig. 5E-H), whereas siRNA-mediated knockdown of *PTGS1* significantly reduced the expression of HBV 3.5-kb RNA, HBeAg, and HBsAg (Fig. 5I-L). These findings establish a direct, positive correlation between *PTGS1* expression and HBV replication.

PTGS1 Suppresses HBV Replication by Modulating the cAMP Synthesis Pathway

To identify the downstream signaling pathways underlying these antiviral effects, intracellular cAMP was quantified using competitive ELISA. Intracellular cAMP levels corresponded with varying concentrations of the HBV plasmid transfected into cells (Fig. 6B-D). As anticipated, COX-1 inhibition decreased the formation of its downstream metabolite thromboxane A_2 (TXA_2), thus relieving the inhibition of adenylate cyclase (AC) and enhancing cAMP synthesis.

Elevated intracellular cAMP activates protein kinase A (PKA), which subsequently phosphorylates the downstream transcription factor CREB. Activation of the PKA–CREB pathway inhibits HBV replication via two mechanisms: firstly, repression of HBV core promoter activity at the transcriptional level, and secondly, impairment of viral core particle assembly at the post-translational stage. The concentration-dependent reductions in *PTGS1* mRNA and HBV 3.5-kb RNA observed in this study align with the inhibitory actions mediated by this signaling pathway.

To directly validate the action of compound triflusal, a treatment group was included in the experiment. Compared to the transfection-only control group, treatment with compound triflusal resulted in significantly higher intracellular cAMP levels (Fig. 6D). Collectively, these data clearly demonstrate that compound triflusal suppresses HBV replication by increasing the activity of the cAMP/PKA/CREB signaling pathway through inhibition of COX-1 expression.

Discussion

This study investigated the anti-HBV activity and underlying mechanism of action of the COX-1 inhibitor, compound triflusal, providing the first evidence of its anti-HBV effects. We identified the cAMP/PKA/CREB signaling pathway as a critical link between COX-1 inhibition and HBV suppression, highlighting a novel direction for developing anti-HBV therapeutic strategies. Experimental data confirmed our hypothesis: within a 0–2 μM concentration range, a linear correlation was observed between *PTGS1* (COX-1), HBV 3.5-kb RNA, and HBV plasmid abundance, indicating that changes in *PTGS1* mRNA levels correlated with antiviral responses. Moreover, HBsAg and HBeAg secretion in cell supernatants increased proportionally with HBV plasmid quantity, confirming that our gradient overexpression system effectively mimics the HBV infection microenvironment. Moreover, targeting COX-1 reversed the enhanced HBV replication induced by high viral loads, suggesting that compound triflusal exhibits sustained inhibitory effects even in high viral replication scenarios, highlighting its therapeutic potential for chronic HBV infections. Mechanistically, compound triflusal reduces thromboxane A_2 (TXA_2) production through COX-1 inhibition, thereby relieving AC inhibition and increasing intracellular cAMP levels. Elevated cAMP further activates the PKA/CREB signaling pathway, suppressing HBV replication at both transcriptional and post-transcriptional stages. Specifically, it inhibits HBV core promoter-mediated 3.5-kb RNA transcription and disrupts HBV core particle assembly and viral capsid formation, ultimately blocking viral maturation and release. This host-targeting antiviral mechanism fundamentally differs from existing nucleos(t)ide analogues that target viral polymerases, representing a novel therapeutic approach. This study elucidates the relationship between COX-1 inhibition and the cAMP signaling pathway in HBV replication. As an established antiplatelet medication, compound triflusal benefits from comprehensive human pharmacokinetic and safety data, potentially enabling direct advancement into HBV efficacy trials without requiring Phase I studies. This significantly reduces the development timeline and associated research costs. Furthermore, its unique host-directed mechanism could demonstrate synergistic effects when combined with existing direct-acting antivirals, potentially overcoming or delaying viral resistance. Crucially, compound triflusal offers dual therapeutic benefits, simultaneously exerting antiplatelet and antiviral effects, particularly advantageous for chronic HBV patients at high cardiovascular thrombotic risk. This dual-action capability simplifies treatment regimens, enhances patient adherence, and promotes overall health.

Conclusion

In summary, we demonstrated that compound triflusal exerts anti-HBV effects in vitro and in vivo by targeting COX-1 to activate the cAMP/PKA/CREB signaling pathway, which suppresses HBV pgRNA transcription and core particle assembly. Gradient overexpression of the HBV plasmid confirmed the dose-dependent regulatory effect of compound triflusal on *PTGS1* expression and HBV replication markers, showing consistent antiviral activity across varying viral loads. Mechanistically, triflusal-mediated COX-1 inhibition reduced TXA_2 generation, elevated intracellular cAMP, and activated the PKA/CREB pathway, suppressing HBV replication at transcriptional and post-transcriptional levels. These findings suggest that COX-1 represents an attractive host target for HBV therapy and provide a theoretical foundation for repurposing compound triflusal for clinical treatment of chronic HBV infection.

Further *in vivo* studies and translational research are warranted to accelerate the clinical application of compound triflusal as an adjunctive anti-HBV drug.

Abbreviations

AC	adenylate cyclase
ATF	activating transcription factor
CHB	chronic hepatitis B
CC_{50}	median cytotoxic concentration
cDNA	complementary DNA
CRE	cAMP response element
CREB	cAMP response element-binding protein
COX-1	cyclooxygenase-1
cAMP	cyclic adenosine monophosphate
DMEM	Dulbecco's Modified Eagle's Medium
DMSO	Dimethyl sulfoxide
ETV	entecavir
ELISA	enzyme-linked immunosorbent assay
FBS	fetal bovine Serum
GAPDH	glyceraldehyde-3-phosphate Dehydrogenase
HBc	Hepatitis B covre Antigen
HBeAg	Hepatitis B e Antigen
HBsAg	hepatitis B surface antigen
HBV	hepatitis B virus
HCCLM3	Hepatocellular Carcinoma with Lymph node Metastasis-3
HDI	hydrodynamic injection
HE	hematoxylin-eosin
HepG2	Human hepatocellular carcinoma cell line G2
Huh7	Human hepatocellular carcinoma cell line 7
HIV	Human Immunodeficiency Virus
HSV-1	herpes simplex virus type 1
HRP	horseradish peroxidase
IHC	immunohistochemical
MTT	3-(4,5-Dimethylthiazol-2-yl)-2,5-diphenyltetrazolium bromide
NC-siRNA	negative control small interfering RNA

OD	optical density
PBS	phosphate-buffered saline
PBST	PBS with Tween-20
PDE	Phosphodiesterase
PKA	protein kinase A
pgRNA	pregenomic RNA
PTGS1	Prostaglandin-Endoperoxide Synthase 1
qPCR	Real-time quantitative PCR
SD	standard deviations
siRNA	small interfering RNA
SPF	Specific Pathogen Free
TDF	tenofovir
TMB	3,3',5,5'-tetramethylbenzidine
TXA_2	thromboxane A_2
WHO	World Health Organization

Declarations

Animal ethics approval

The animal experiments had the approval of the Animal Care and Use Committee of the Wuhan Institute of Virology (WIVA38202103).

Consent for publication

All authors have read and agreed to the final version of the manuscript.

Availability of data and materials

The datasets used and/or analyzed during the current study are available from the corresponding author on reasonable request.

Competing interests

The authors declare no competing interests.

Funding

This research was supported by grant from the Hubei natural science foundation (No. ZRMS2023001990), the Wuhan Science and Technology Bureau (No. 2023020201010211), and the grants from the National Natural Science Foundation of China (No. 32200134) and the State Key Laboratory for Diagnosis and Treatment of Severe Zoonotic Infectious Diseases (No. 2024KF00005). All data are presented in the article or attachments.

Authors' contributions

†Huijing Ruan (H.R.), Kai Yang (K.Y.), and Mingzhe Yan (M.Y.) contributed equally to this work.

H.R., K.Y., and M.Y. performed the majority of the experiments, analyzed the data, and drafted the original manuscript.

Xiaojian Tan (X.T.), Wenyuan Zhang (W.Z.), Jie Zhou (J.Z.), and Bei Ye (B.Y.) assisted with the in vitro and in vivo experiments, virus preparation, and data validation.

Jisong Yan (J.Y.) provided critical reagents and contributed to the study design.

Qingyu Yang (Q.Y.), Jie Xiang (J.X.), and Lianguo Ruan (L.R.) supervised the study, secured funding, revised the manuscript, and provided intellectual guidance.

All authors have read and approved the final version of the manuscript.

Acknowledgements

The authors express gratitude to Dr. Jianguo Wu (Wuhan Institute of Virology, Chinese Academy of Sciences, Wuhan, China) for graciously providing the HBV1.3 plasmid.

References

1. Xu R, Zhang L, Wang Y, et al. Advances in HBV infection and replication systems in vitro. Virol J. 2021;18:105. https://doi.org/10.1186/s12985-021-01626-4
2. Zoulim F, Chen PJ, Dandri M, Kennedy PT, Seeger C. Hepatitis B virus DNA integration: Implications for diagnostics, therapy, and outcome. J Hepatol. 2024;81:1087-1099. https://doi.org/10.1016/j.jhep.2024.03.014
3. Yan R, Li J, Zhang H, et al. 2024 latest report on hepatitis B virus epidemiology in China: Current status, changing trajectory, and challenges. Hepatobiliary Surg Nutr. 2025;14:66-77. https://doi.org/10.1016/j.hbsn.2024.11.005
4. Hui Z, Wang S, Liu X, et al. New progress in HBV control and the cascade of health care for people living with HBV in China: Evidence from the fourth national serological survey, 2020. Lancet Reg Health West Pac. 2024;51:101193. https://doi.org/10.1016/j.lanwpc.2024.101193

5. Deng Y, Meng T, You H, Jia J, Wang Y. Epidemiology, achievements, and challenges in the elimination of hepatitis B in China. J Clin Transl Hepatol. 2025;13:1-9. https://doi.org/10.1016/j.jcth.2024.12.002
6. Marcellin P, Heathcote EJ, Buti M, Gane E, de Man RA, Krastev Z, et al. Tenofovir disoproxil fumarate versus adefovir dipivoxil for chronic hepatitis B. N Engl J Med. 2008;359(23):2442-2455. https://doi.org/10.1056/NEJMoa0802878
7. Lok ASF, Lai CL, Leung N, Yao G, Guan R, Sung JJ. Evolution of hepatitis B virus polymerase gene mutations in hepatitis B E antigen-negative patients receiving lamivudine therapy. Hepatology. 2000;32(6):1145-1153.
8. Casado JL. Renal and bone toxicity with the use of tenofovir: Understanding at the end. AIDS Rev. 2016;18(4):205-217.
9. Wong GLH, Gane E, Lok ASF. How to achieve functional cure of HBV: Stopping NUCs, adding interferon or new drug development? J Hepatol. 2022;76(6):1249-1262.
10. Lok ASF. Toward a functional cure for hepatitis B. Gut Liver. 2024;18(4):593-601.
11. Anninos H, Gougos A, Vasiliadis T, Hadjidis N. Triflusal: An old drug in modern antiplatelet therapy. Review of its action, use, safety and effectiveness. Hellenic J Cardiol. 2009;50(3):199-207.
12. De La Cruz JP. Triflusal. Drugs. 1998;55(6):834.
13. De Miguel LS, López-Farré A, Alvarez-Sala A, Miró-Casas E, De La Cruz JP. A 4-trifluoromethyl derivative of salicylate, triflusal, stimulates nitric oxide production by human neutrophils: role in platelet function. Eur J Clin Invest. 2000;30(9):811-817.
14. De La Cruz JP, Villalobos MA, García PJ, Smith-Agreda JM, Sánchez de la Cuesta F. Effects of triflusal and its main metabolite HTB on platelet interaction with subendothelium in healthy volunteers. Eur J Clin Pharmacol. 1995;47(5):497-502.
15. Montero Domínguez M, González B, Zimmer J. Neuroprotective effects of the anti-inflammatory compound triflusal on ischemia-like neurodegeneration in mouse hippocampal slice cultures occur independent of microglia. Exp Neurol. 2009;218(1):11-23.
16. Rodriguez G, Ross JA, Nagy ZS, Kirken RA. Forskolin-inducible cAMP pathway negatively regulates T-cell proliferation by uncoupling the interleukin-2 receptor complex. J Biol Chem. 2013;288(10):7137-7146.
17. López-Abente J, Correa-Rocha R, Pion M. Functional mechanisms of Treg in the context of HIV infection and the janus face of immune suppression. Front Immunol. 2016;7:192. https://doi.org/10.3389/fimmu.2016.00192
18. Tacke F, Liedtke C, Bocklage S, Manns MP, Trautwein C. CREB/PKA sensitive signalling pathways activate and maintain expression levels of the hepatitis B virus pre-S2/S promoter. Gut. 2005;54(9):1309-1317.
19. Ray N, Enquist LW. Transcriptional response of a common permissive cell type to infection by two diverse alphaherpesviruses. J Virol. 2004;78(7):3489-3501.

20. Carey MA, Asselin-Paturel C, Boivin G, Girard M, Lemire M, Perreault S, et al. Pharmacologic inhibition of COX-1 and COX-2 in influenza A viral infection in mice. PLoS One. 2010;5(6):e11610. https://doi.org/10.1371/journal.pone.0011610
21. Whitehead S, Cheng G, Hachinski V, Cechetto DF. Interaction between a rat model of cerebral ischemia and β-amyloid toxicity: II. Effects of triflusal. Stroke. 2005;36(8):1782-1789.
22. Zhou M, Yi M, Zhang Y, Liu Y, Yan H, Gao Z, et al. Productive HBV infection of well-differentiated, hNTCP-expressing human hepatoma-derived (Huh7) cells. Virol Sin. 2017;32(6):465-475.
23. Schicht G, Seidemann L, Haensel R, Seehofer D, Damm G. Critical investigation of the usability of hepatoma cell lines HepG2 and Huh7 as models for the metabolic representation of resectable hepatocellular carcinoma. Cancers. 2022;14(17):4227. https://doi.org/10.3390/cancers14174227
24. Huang X, Ma J, Xu J, Su Q, Zhao J. Simvastatin induces growth inhibition and apoptosis in HepG2 and Huh7 hepatocellular carcinoma cells via upregulation of Notch1 expression. Mol Med Rep. 2015;11(3):2334-2340. https://doi.org/10.3892/mmr.2014.3047
25. Murayama A, Akari H, Kato T. Production and purification of cell culture-generated hepatitis B virus by transient transfection and density gradient. Bio-protocol. 2023;13(12). https://doi.org/10.21769/BioProtoc.4614
26. Paturel A, Lemoine M, Abadie V, Garin-Chalandre A, Saillard C, Ganne-Carrié N, et al. A molecular standard for circulating HBV RNA detection and quantification assays in patients with chronic hepatitis B. JHEP Rep. 2024;6(5):101124. https://doi.org/10.1016/j.jhepr.2024.101124
27. Song Y, Zhang Y, Li X, Wang X, Chen Y, Liu J, et al. Establishment and characterization of a new cell culture system for hepatitis B virus replication and infection. Virol Sin. 2022;37(3):558-568.
28. Ongrádi J, Telekes A. Relationship between the prostaglandin cascade and virus infection. Acta Virol. 1990;34(6):380-400.

Figures

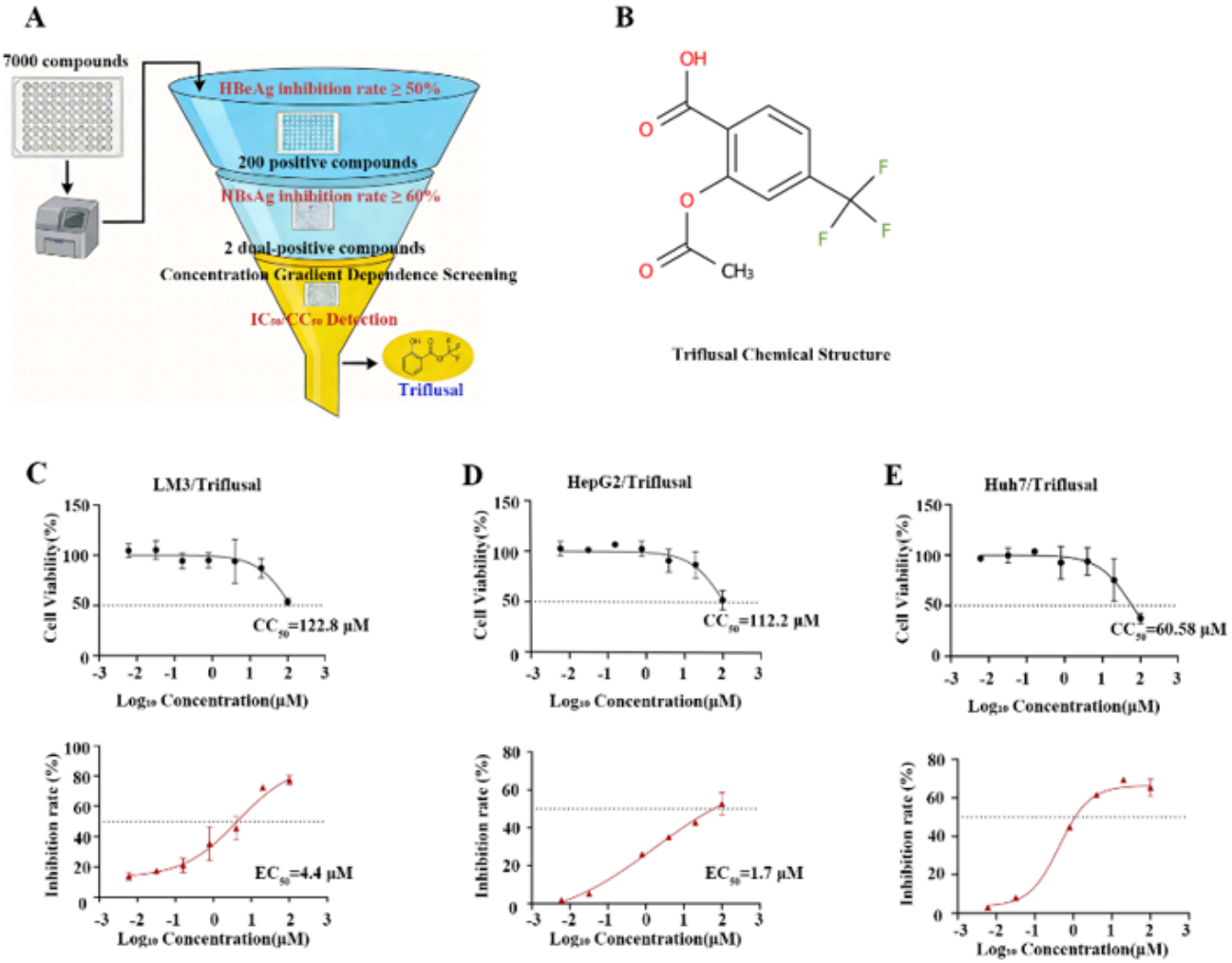


Figure 1

The HepG2.2.15 cell line is suitable for screening compounds that inhibit HBV replication.

(A) Schematic workflow of compound screening. (B) Chemical structure of GSK583. Cytotoxicity of triflusal in Huh7, HepG2 and LM3 cells was detected by MTT assay.

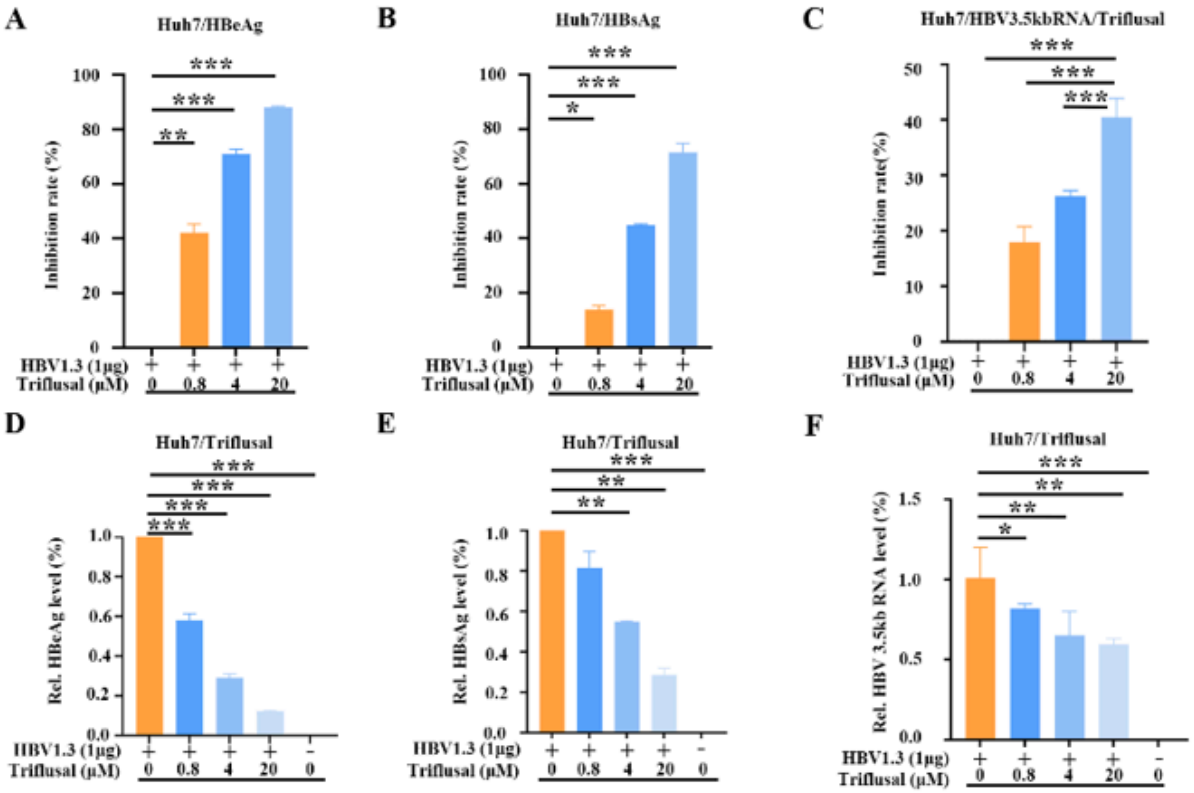


Figure 2

In vitro suppression of HBV by triflusal.

Huh7 cells were untransfected or transfected with 1 μg HBV1.3, then treated with serially diluted triflusal (0.8, 4, 20 μM) for 30 h. HBV 3.5 kb mRNA level was detected by qPCR (A). HBeAg and HBsAg levels were measured by ELISA (B, C), and inhibition rates were calculated (D-F). *p < 0.05, **p < 0.01, ***p < 0.001.

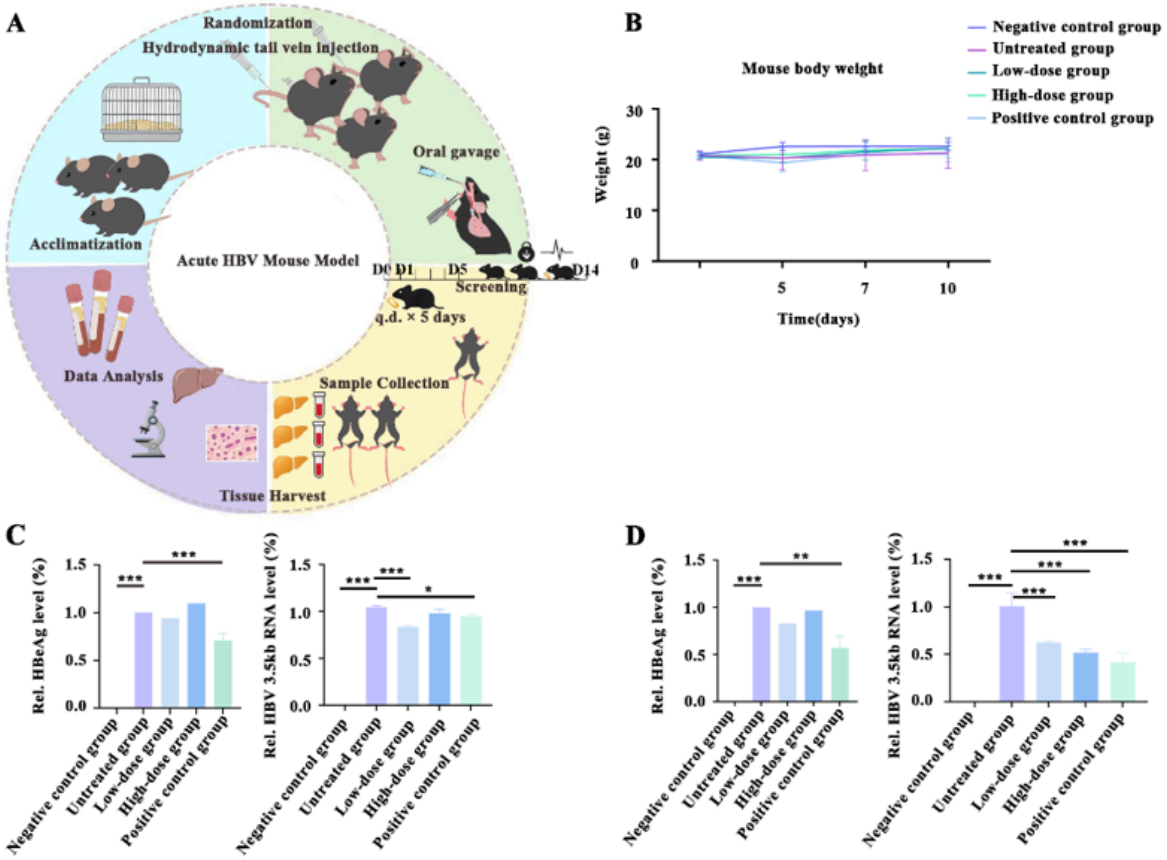


Figure 3

In vivo suppression of HBV by triflusal.

(A) Schematic of the HBV mouse infection model. Six-to seven-week-old male C57BL/6 mice received hydrodynamic injection (HDI) of pAAV/HBV1.2 plasmid via tail vein, then were treated with triflusal (30-50 mg/kg) or vehicle once daily for 5 days. (B) Body weight changes of mice in each group. (C) Paraffin sections of liver and blood tissues from normal control, untreated and triflusal-treated mice at 5 and 14 days post-infection. (D) Hepatic HBV 3.5 kb mRNA level detected by qPCR. (E) Serum HBeAg level measured by ELISA. *p < 0.05, **p < 0.01, ***p < 0.001.

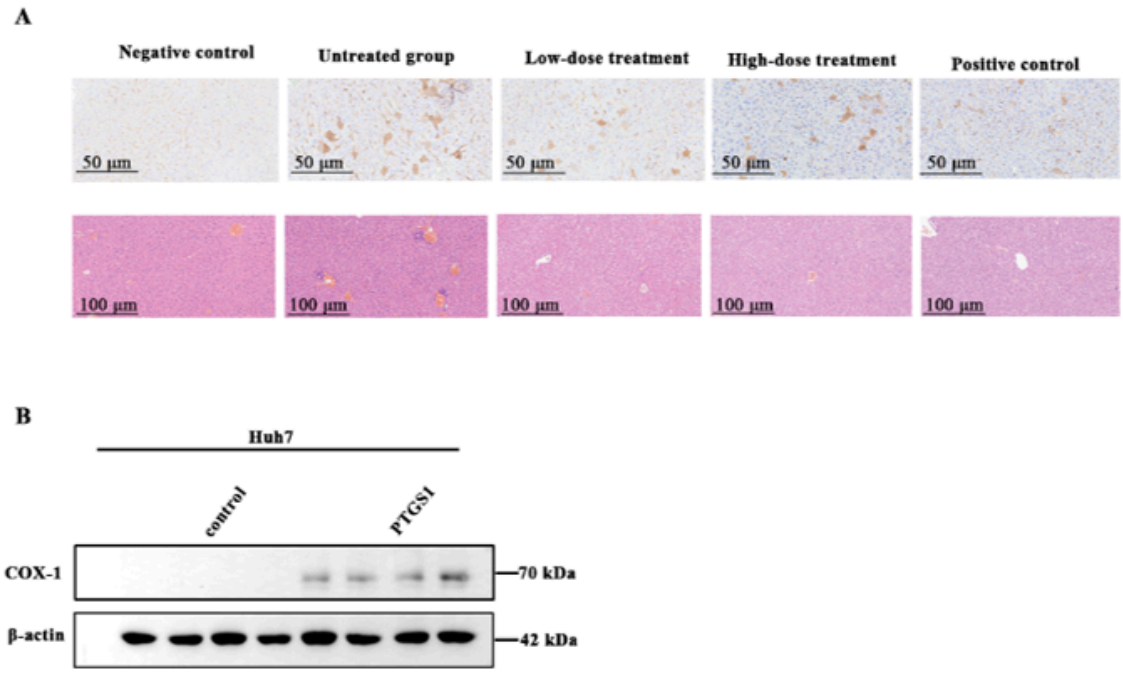


Figure 4

Triflusal modulates liver histopathology and *PTGS1*/COX-1 expression.

(A) Representative images of mouse liver sections. Upper: Immunohistochemical (IHC) staining for HBV-related antigen (scale bar, 50 μm). Lower: Hematoxylin-eosin (HE) staining (scale bar, 100 μm). Groups: negative control, HBV model (untreated), low-dose triflusal, high-dose triflusal, positive control. Liver pathological changes were analyzed by HE staining, and hepatic HBc level was detected by IHC. (B) Western blot analysis of COX-1 (*PTGS1*-encoded) expression in Huh7 cells transfected with empty vector or *PTGS1*overexpression vector. β-actin was used as the loading control.

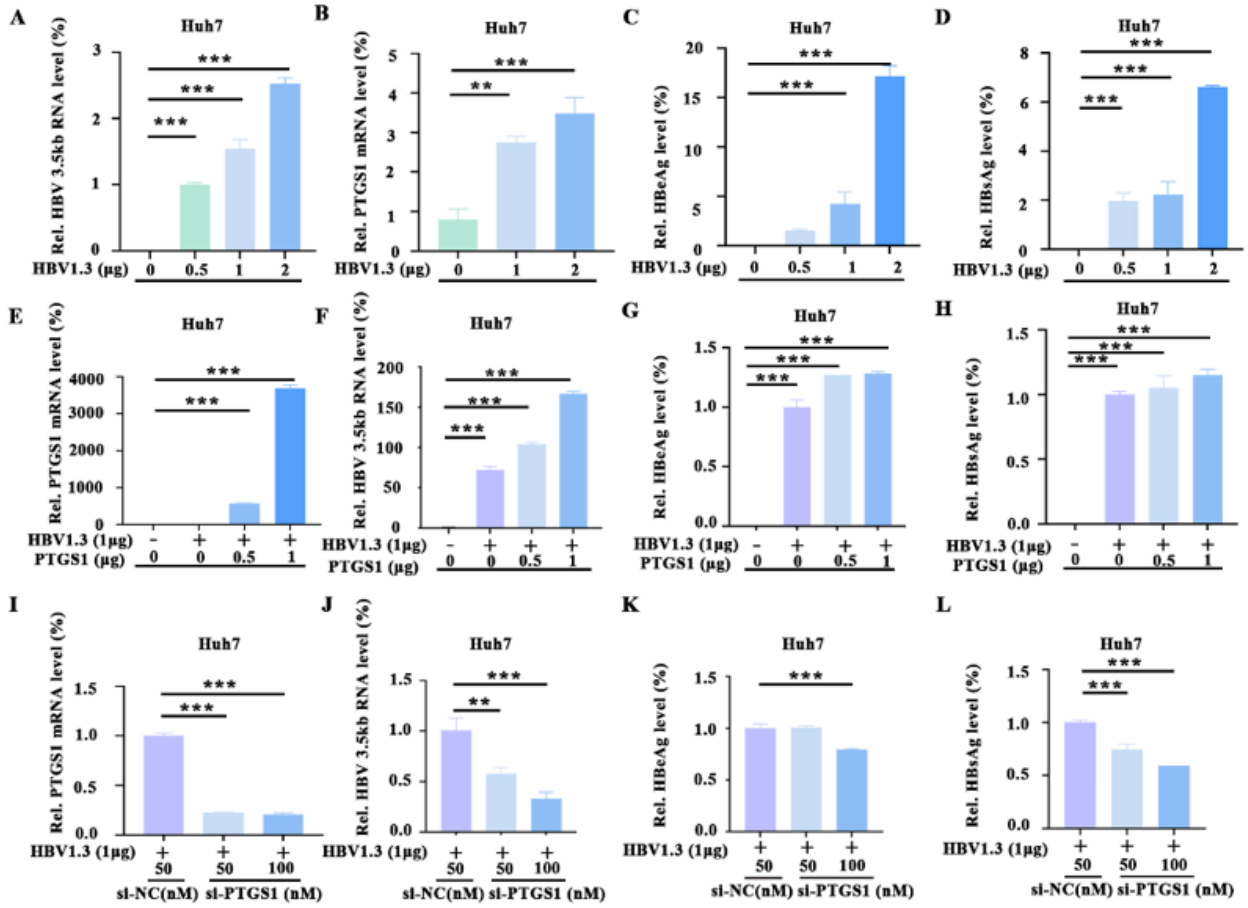


Figure 5

The role of *PTGS1* in triflusal-mediated HBV suppression.

Huh7 cells were untransfected or transfected with 0, 0.5, 1 μg HBV1.3 for 60 h: *PTGS1*level by qPCR (A), HBV 3.5 kb mRNA level by qPCR (B), HBeAg, HBsAg and cAMP levels by ELISA (C-D). Huh7 cells were untransfected or transfected with 1 μg HBV1.3, then treated with 0, 0.5, 1 μg *PTGS1* for 60 h: *PTGS1*level by qPCR (E), HBV 3.5 kb mRNA level by qPCR (F), HBeAg and HBsAg levels by ELISA (G-H). Huh7 cells were untransfected or transfected with 1 μg HBV1.3, then co-transfected with si-*PTGS1* for 60 h: *PTGS1* level by qPCR (I), HBV 3.5 kb mRNA level by qPCR (J), HBeAg and HBsAg levels by ELISA (K-L). *p < 0.05, **p < 0.01, ***p < 0.001. All experiments were independently repeated three times.

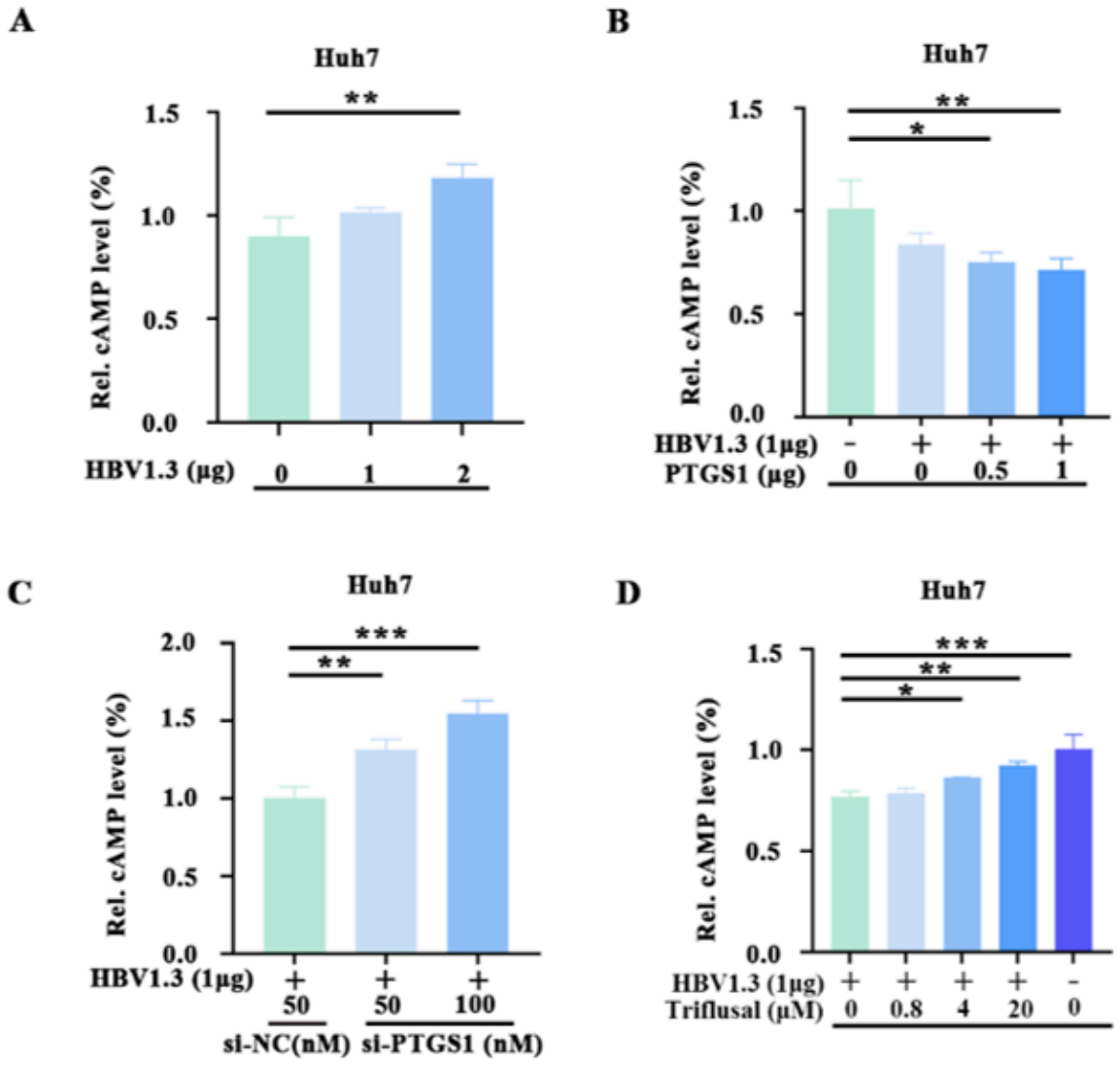


Figure 6

PTGS1 inhibits HBV replication by blocking cAMP synthesis pathway.

(A) Huh7 cells were untransfected or transfected with 0, 0.5, 1 μg HBV1.3 for 60 h; cAMP level was measured by ELISA. (B) Huh7 cells were untransfected or transfected with 1 μg HBV1.3, then treated with 0, 0.5, 1 μg *PTGS1* for 60 h; cAMP level was measured by ELISA. (C) Huh7 cells were untransfected or transfected with 1 μg HBV1.3, then co-transfected with si-*PTGS1*for 60 h; cAMP level was measured by ELISA. (D) Huh7 cells were untransfected or transfected with 1 μg HBV1.3, then treated with serially diluted triflusal (0.8, 4, 20 μM) for 60 h; cAMP level was measured by ELISA. *p < 0.05, **p < 0.01, ***p < 0.001. All experiments were independently repeated three times.

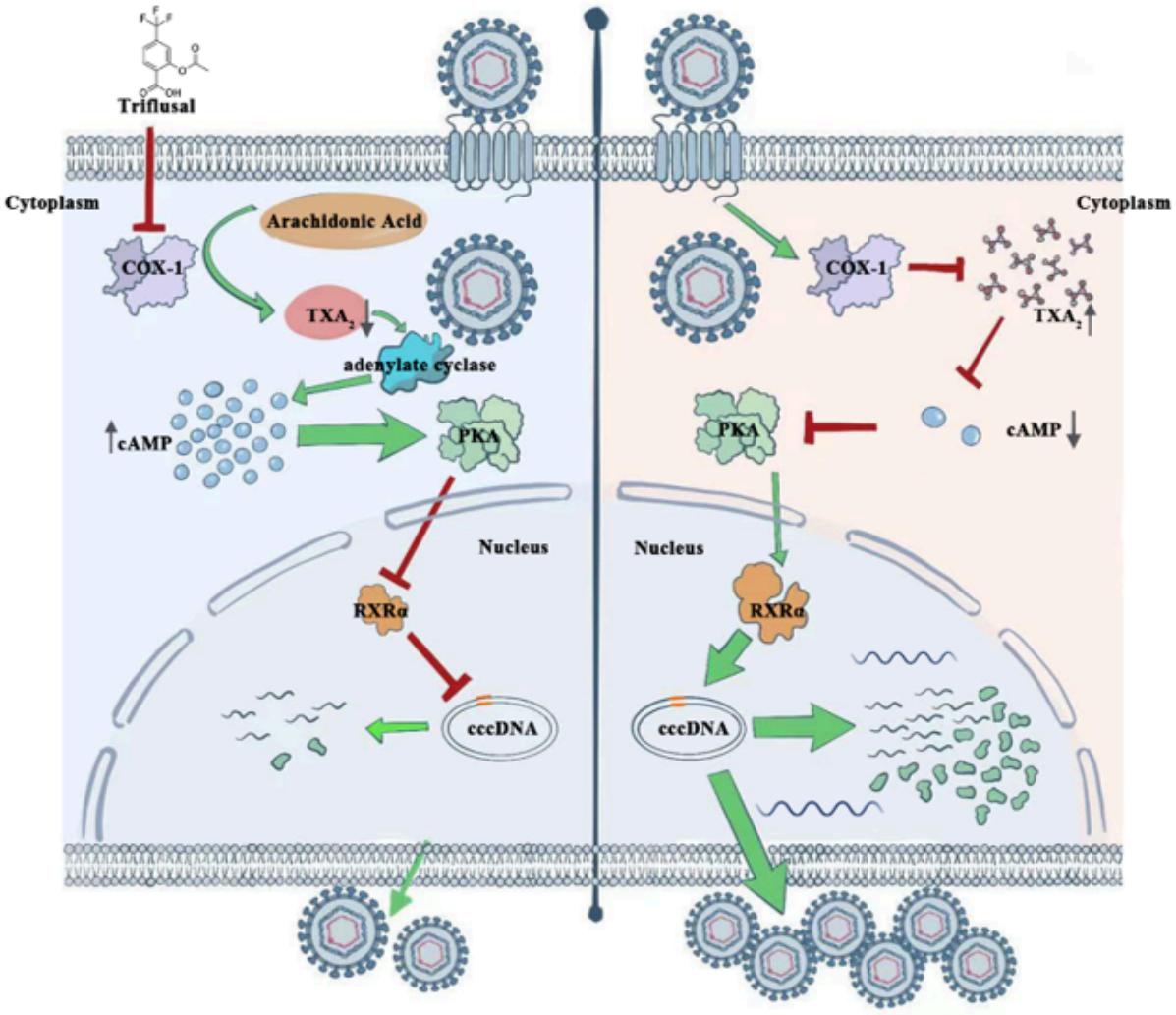


Figure 7

Proposed mechanism of triflusal for inhibiting HBV replication.

HBV invades host cells via the sodium taurocholate cotransporting polypeptide (NTCP) receptor. Triflusal regulates intracellular cyclic adenosine monophosphate (cAMP) by two pathways: (1) directly inhibiting cyclooxygenase-1 (COX-1) to reduce thromboxane A_2 (TXA_2) synthesis, and the decreased TXA_2 further stimulates adenylate cyclase to promote cAMP production; (2) inhibiting phosphodiesterase (PDE) activity to reduce cAMP degradation. Accumulated cAMP activates protein kinase A (PKA), which induces phosphorylated cAMP response element binding protein (p-CREB) to repress retinoid X receptor alpha (RXRα), thereby blocking hepatitis B virus covalently closed circular DNA (cccDNA) transcription and viral RNA production. Additionally, activated PKA disrupts downstream processes including HBV core protein synthesis, capsid assembly and mature virion exocytosis, ultimately inhibiting HBV replication and propagation.

Supplementary Files

This is a list of supplementary files associated with this preprint. Click to download.

- 2025Huh7HBVptgs1110B.xlsx
- 20250415HUN7HBV3.5kbRNARTQPCR.xlsx
- 20250418Huh7PTGS1.xlsx
- 20251112huh7hbvptgs1cv01.xlsx
- 20251017Huh7HBV02.xlsx
- 20251206HBVSIRNA1123YANG.xlsx
- 20251211HBV1017YANG.xlsx
- 20260112coxactin.tif